An electron paramagnetic resonance study of Mn-doped $Bi_4Ge_3O_{12}$

1990 J. Phys.: Condens. Matter 2 10123

(http://iopscience.iop.org/0953-8984/2/50/016)

J. Phys.: Condens. Matter 2 (1990) 10123–10130. Printed in the UK

An electron paramagnetic resonance study of Mn-doped $Bi_4Ge_3O_{12}$

D Bravo†, L Arizmendi†, M Aguilar‡ and F J López†

† Departamento de Física Aplicada C-IV, Universidad Autónoma de Madrid, Cantoblanco, E-28049 Madrid, Spain

‡ Instituto de Ciencia de Materiales, Consejo Superior de Investigaciones Científicas, Universidad Autónoma de Madrid, Cantoblanco, E-28049 Madrid, Spain

Received 31 May 1990, in final form 23 July 1990

Abstract. Electron paramagnetic resonance spectroscopy of Mn-doped $Bi_4Ge_3O_{12}$ single crystals has been studied at room temperature in the X band. The spectra obtained have been attributed to Mn^{2+} ions in the Bi^{3+} site without local charge compensation having trigonal symmetry. Moreover, the spin-Hamiltonian parameters have been interpreted by means of the superposition model in order to obtain information about the relaxation of the lattice in the neighbourhood of the impurity.

1. Introduction

Single crystals of $Bi_4Ge_3O_{12}$ have attracted considerable attention owing to their applications as scintillators [1] and non-linear optical devices [2] and for their potential as solid state laser host [3]. Also, photorefractive properties have been described recently for single crystals doped with Cr ions [4].

However, few works have appeared devoted to $Bi_4Ge_3O_{12}$ doped with iron-group transition ions. A study of the position of doping ions in the host, as well as their charge state, should be relevant for optimizing the above-mentioned applications. In particular, the iron-group transition ions are expected to be relevant as charge traps involved in the photorefractive properties of $Bi_4Ge_3O_{12}$ [4] in the same way as they have proved to be in other photorefractive crystals [5, 6]. In particular, the role of these ions in $Bi_{12}GeO_{20}$, the 6:1 stoichiometry of BiGeO is not yet established.

$Bi_4Ge_3O_{12}$ belongs to the crystalline symmetry groups $\bar{4}3m$ [7] and the unit cell has four chemical formulae, i.e. a total of 76 atoms. This structure, known as eulytite, is formed by a cubic arrangement of oxygen-distorted octahedra surrounding each Bi^{3+} ion and oxygen tetrahedra surrounding each Ge^{4+} ion [8]. The tetrahedron around the Ge^{4+} is slightly distorted along the $\langle 100 \rangle$ directions. On the other hand, the four $\langle 111 \rangle$ directions of the cubic cell are C_3 axes for the Bi^{3+} sites. The six oxygen ions around the Bi^{3+} site form two different equilateral triangles, so that there are three oxygen ions at a distance $R_a = 2.149$ Å forming an angle θ_a of 51.38° with the C_3 axis and three others at a distance $R_b = 2.620$ Å forming an angle θ_b of 104.62°.

The luminescence of Mn-doped $Bi_4Ge_3O_{12}$ ($Bi_4Ge_3O_{12}:Mn^{2+}$) single crystals has been studied recently in [9] and interpreted as due to Mn^{2+} ions in a cubic crystal field.

0953-8984/90/5010123 + 08 $03.50

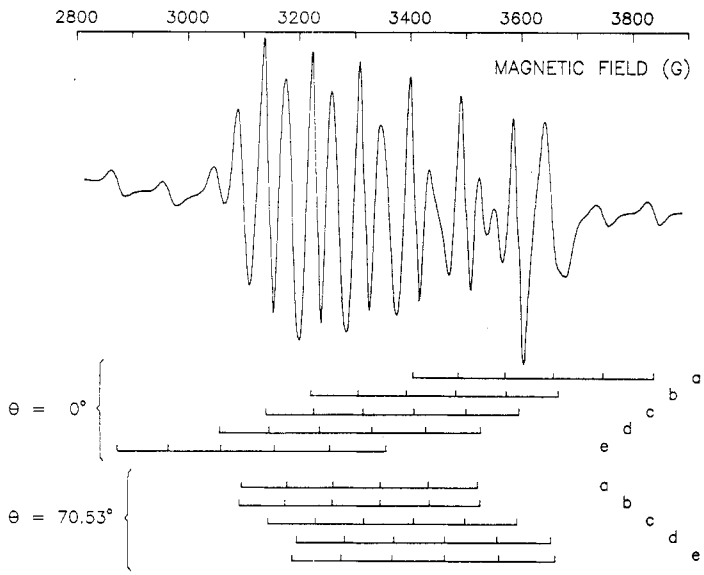

Figure 1. EPR spectrum of a Mn-doped $Bi_4Ge_3O_{12}$ sample, measured at room temperature, with the external magnetic field along a ⟨111⟩ direction. The lower part of the figure shows the calculated resonance fields for the defects whose axis form an angle of 0° and 70.53° with $\boldsymbol{H}$. The labels a, b, c, d and e indicate the electronic transitions $[\frac{5}{2}\rangle \rightarrow [\frac{3}{2}\rangle$, $[\frac{3}{2}\rangle \rightarrow [\frac{1}{2}\rangle$, $[\frac{1}{2}\rangle \rightarrow [-\frac{1}{2}\rangle$, $[-\frac{1}{2}\rangle \rightarrow [-\frac{3}{2}\rangle$ and $[-\frac{3}{2}\rangle \rightarrow [-\frac{5}{2}\rangle$, respectively.

It is well known that this ion yields a magnetic resonance spectrum with both fine and hyperfine structure that gives information about its environment. Thus, in order to confirm the valence state of manganese in $Bi_4Ge_3O_{12}$ and to clarify its location in the lattice, we have performed a study of the electron paramagnetic resonance (EPR) spectrum of the same crystals used in [9]. Also, the lattice relaxation around the impurity has been discussed using the superposition model.

2. Experimental details

Single crystals of $Bi_4Ge_3O_{12}$ were grown in our laboratory by the Czochralski technique. Bi_2O_3 and GeO_2 powders (Puratronic Johnson–Matthey) were mixed in the molar proportions 2:3 and melted in a platinum crucible under a pure oxygen atmosphere at 1.1 atm. Manganese doping was achieved by adding MnO powder (grade R from Merck) to the melt in a concentration of 0.1 mol%. The pulling direction was chosen along one of the cubic axes ⟨100⟩. From the boule obtained, samples of 2 mm × 2 mm × 8 mm were sawn with their faces perpendicular to ⟨100⟩ directions as determined by taking a number of Laue x-ray diffraction patterns.

The EPR spectra were obtained with a Varian E-12 spectrometer in the X band with a field modulation frequency of 100 kHz at room temperature. Accurate values of the resonance magnetic fields and microwave frequencies were measured with a Bruker NMR gaussmeter (model ER 035 M) and a Hewlett–Packard frequency meter (model

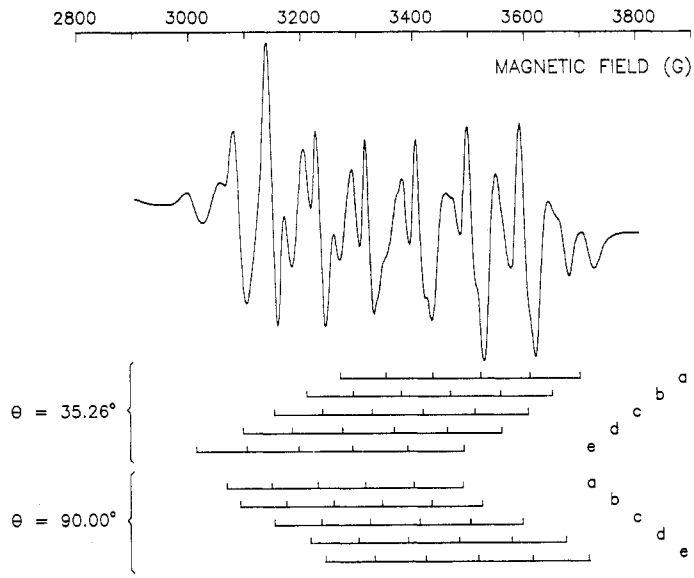

Figure 2. EPR spectrum, measured at room temperature, with the external magnetic field along a ⟨110⟩ direction, of a Mn-doped $Bi_4Ge_3O_{12}$ sample. The lower part of the figure shows the calculated resonance fields for the defects whose axis form an angle of 35.26° and 90° with $\boldsymbol{H}$.

5342A) respectively. The sample was placed in a home-made two-axis goniometer, so that it could be rotated in two perpendicular planes.

3. Results

The EPR spectrum of $Bi_4Ge_3O_{12}:Mn^{2+}$ samples consists of two well differentiated regions. There is a group of intense lines near 3200 G ($g_{eff} \simeq 2$) which is shown in figures 1–3 for different orientations of the magnetic field $\boldsymbol{H}$; and another much weaker (about 100 times) group of lines near 1600 G ($g_{eff} \simeq 4$). Both groups are composed of sextets of lines with a separation between lines of about 90 G, which is the characteristic hyperfine structure of the Mn^{2+} ions.

There is a strong overlapping of the various sextets in the spectra. This fact (and the large peak-to-peak linewidth, which is about 20 G) makes it very difficult to ascertain the exact position of each line except for a few at both extremes of the spectra. Also, it makes it impossible to follow the whole angular variation of the spectrum. However, it is observed that various sets of lines collapse, and the spectrum becomes simpler, when $\boldsymbol{H}$ is along the main crystallographic directions ⟨100⟩, ⟨110⟩ and ⟨111⟩. Therefore, the orientations of the main axis of the defect must be symmetric with respect to those crystallographic directions.

The EPR spectra in the $g_{eff} \simeq 2$ region, measured at room temperature, of a $Bi_4Ge_3O_{12}:Mn^{2+}$ sample obtained with $\boldsymbol{H}$ parallel to the ⟨111⟩, ⟨110⟩ and ⟨100⟩ crystallographic directions are given in figures 1, 2 and 3, respectively. It was ascertained that the maximum splitting of the spectrum takes place when $\boldsymbol{H}$ is parallel to a ⟨111⟩ axis. Therefore, these directions were chosen as the main axis for the defect. On the other

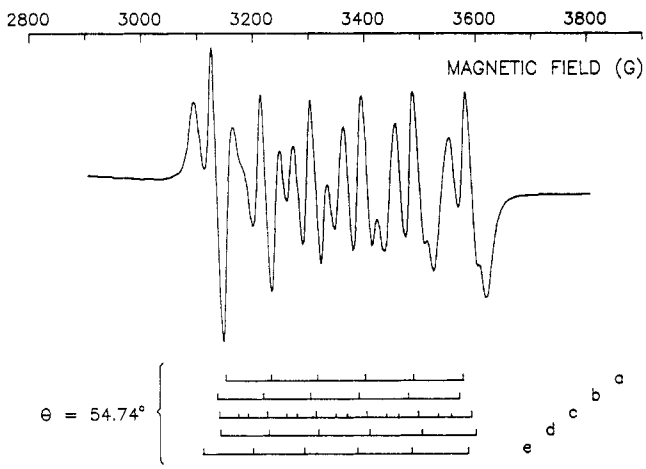

Figure 3. EPR spectrum, measured at room temperature, with the external magnetic field along a ⟨100⟩ direction, of a Mn-doped $Bi_4Ge_3O_{12}$ sample. The lower part of the figure shows the calculated resonance fields for the defects whose axis form an angle of 54.74° with $\boldsymbol{H}$. In the $[\frac{1}{2}\rangle \rightarrow [-\frac{1}{2}\rangle$ electronic transition, the 'forbidden' nuclear transitions are also indicated by short bars.

hand, the spectrum obtained with $\boldsymbol{H}$ parallel to a ⟨100⟩ axis shows a small splitting. This behaviour is consistent with defects having axial symmetry along the ⟨111⟩ axes. In this case, when the magnetic field is applied along a ⟨111⟩ direction, there are two orientations of the defects, i.e. one with the field at 0° and another with the field at 70.53° which is threefold degenerate. If $\boldsymbol{H}$ is along a ⟨110⟩ direction, there are two orientations, both twofold degenerate, with the field at 35.26° and at 90°. Finally, when $\boldsymbol{H}$ is along a ⟨100⟩ direction, all the orientations of the centres are equivalent, forming an angle of 54.74° with the field.

Owing to the $3d^5$ configuration of the Mn^{2+} ion, the ground state is $^6S_{5/2}$ and the effective spin Hamiltonian appropriate for the analysis of a trigonal site is

$$\hat{\mathcal{H}} = g_{\parallel}\beta H_z\hat{S}_z + g_{\perp}\beta(H_x\hat{S}_x + H_y\hat{S}_y) + B_2^0\hat{O}_2^0 + B_4^0\hat{O}_4^0 + B_4^3\hat{O}_4^3 + A_{\parallel}\hat{S}_z\hat{I}_z + A_{\perp}(\hat{S}_x\hat{I}_x + \hat{S}_y\hat{I}_y) - g_N\beta_N\boldsymbol{H}\cdot\hat{I}$$

where x, y and z are the defect axes system, $S = \frac{5}{2}$ and $I = \frac{5}{2}$.

A first analysis of the spectra was made using a perturbation calculation, because the Zeeman term is dominant compared with the other terms. These approximate values were used as the initial values for the parameters of a fitting process which is carried out by numerical diagonalization of the energy matrices by Jacobi's method, so that eigenvalues as well as eigenfunctions were obtained. A minimization subroutine gave the 30 resonance fields for a given set of parameters and for each orientation of the defect axis with respect to the magnetic field. As the hyperfine term involves an energy comparable with those of crystal-field terms, the complete matrix 36×36 should be diagonalized. The best set of spin-Hamiltonian parameters obtained with this fitting are given in table 1. Here the sign of the parameters was determined from the assumption that $A < 0$. The calculated resonance field values corresponding to the different orientations of defects when $\boldsymbol{H}$ is parallel to the ⟨111⟩, ⟨110⟩ and ⟨100⟩ crystallographic directions are included in figures 1, 2 and 3 as stick diagrams for comparison. It is

Table 1. Spin-Hamiltonian parameters for Mn^{2+} in $Bi_4Ge_3O_{12}$. The B_n^m coefficients are related to the other usual crystal-field parameters as follows: $D = b_2^0 = 3B_2^0$, $b_4^m = 60B_4^m$, $a = -(9/\sqrt{2})B_4^3$, $a - F = -180B_4^0$.

$g_\parallel = g_\perp$	1.9985 ± 0.0005
B_2^0 (10^{-4} cm^{-1})	-17.4 ± 0.1
B_4^0 (10^{-4} cm^{-1})	-0.113 ± 0.002
B_4^3 (10^{-4} cm^{-1})	-1.8 ± 0.2
$A_\parallel$ (10^{-4} cm^{-1})	-85.0 ± 0.1
$A_\perp$ (10^{-4} cm^{-1})	-83.2 ± 0.7

observed that the agreement with the experimental lines is very good taking into account the width of the lines and the strong overlapping.

The much weaker spectra in the $g_{\text{eff}} \simeq 4$ region can be interpreted as due to forbidden transitions with $\Delta M > 1$. The eigenfunctions of the spin Hamiltonian obtained at about 1600 G show a strong mixing of eigenfunctions of angular momenta due to the similar magnitudes of the various terms in the Hamiltonian, so that forbidden nuclear transitions ($\Delta m \neq 0$) are also possible for all orientations of the magnetic field. However, the transition probability is higher when $\boldsymbol{H}$ is along a $\langle 100 \rangle$ direction.

If we recall the distribution of the oxygen ions around the Ge^{4+} and Bi^{3+} sites mentioned in section 1, the axial symmetry along the $\langle 111 \rangle$ directions for the defects related to Mn^{2+} ions can be explained assuming that Mn^{2+} ions substitute for the Bi^{3+} ions, because only the Bi^{3+} sites have such symmetry. This is a result similar to that obtained for Gd^{3+}-doped crystals [10] and is in agreement with the results of luminescence obtained from the same crystals [9]. The Mn^{2+} ions could have local charge compensation by an ion along the $\langle 111 \rangle$ direction that would still maintain the same symmetry. As the $\langle 111 \rangle$ direction is occupied only by Bi^{3+} ions, one could consider that a diamagnetic impurity with valence 4+ substitutes for a Bi^{3+} in the neighbourhood of the Mn^{2+} ion. However, it is more likely that the charge compensation is of non-local type as in other oxides [11].

4. Discussion

Since the first observation of the hyperfine interaction of a divalent manganese impurity in a solid in 1951, a large number of papers on this ion in different crystals have been published. In particular, Van Wieringen [12] showed that the hyperfine splitting A depends on the host lattice. This parameter A was related to the bonding in a phenomenological way by Matumura [13] by plotting A versus Pauling's covalency parameter per ligand. Later, Simánek and Müller [14] explained this relationship as due to the dominance of the 4s bonding of the impurity over the 3d bonding.

From the experimental values of the hyperfine parameters $A_\parallel$ and $A_\perp$ the isotropic and anisotropic contributions to the hyperfine interaction can be calculated. The isotropic contribution $A_s = (A_\parallel + 2A_\perp)/3$ is related to the overlap between the oxygen and paramagnetic ion orbitals, i.e. to the covalency, and is the important parameter in our discussion.

The value obtained in our case is $A_s = -83.8(\pm 0.5) \times 10^{-4}\ cm^{-1}$. From the phenomenological curve of Matumura updated by Simánek and Müller we can see that this value corresponds to a c/n-value of about 9%. As the number of ligands n is 6, the covalency parameter c is 54%. Thus, the number of ligands is the same as in simple oxides and the covalency parameter is very close to those obtained for Mn in MgO, CaO and SrO [14]. In these oxides the Mn–O distance lies in the range 2.14–2.4 Å [15]; thus a distance R_b = 2.62 Å for half of the ligands in $Bi_4Ge_3O_{12}$ is quite unlikely. It is reasonable to think that the distance is closer to that for the above-mentioned oxides, i.e. an appreciable relaxation of these oxygen ions towards the Mn^{2+} ion is expected.

In order to obtain further insight about the positions of the oxygen ligands, we have used the superposition model in [16, 17]. In this model, each spin-Hamiltonian parameter is constructed from the superposition of single-ligand contributions. The model has been successfully tested for rare-earth impurities and extended to $3d^5$ impurities. In particular, the Mn^{2+} case with oxygen ligands has been studied by Newman and Siegel [18], Siegel and Müller [19] and Rubio *et al* [15].

The superposition model assumes that the spin-Hamiltonian parameters b_n^m result from a linear superposition of the form

$$b_n^m = \sum \bar{b}_n(R_i) K_n^m(\theta_i, \varphi_i)$$

where the $K_n^m(\theta_i, \varphi_i)$ are spherical harmonic functions of rank n of the polar angles which define the position of each ligand and the $\bar{b}_n(R)$ are functions of the radial metal–ligand distance R and are known as intrinsic parameters. On the other hand, the model proposes that the functional form of the $\bar{b}_n(R)$ intrinsic parameters obeys a single potential law

$$\bar{b}_n(R_i) = \bar{b}_n(R_0)(R_0/R_i)t_n$$

where R_0 is a reference distance and R_i the distance of the ligand ion i. Thus a first problem in the application of the model is to obtain accurate values of the different t_n (in our case t_2 and t_4) and of $\bar{b}_n$ for a given distance.

With regards to t_4, Newman and Siegel [18] use a value of 7, but later Rubio *et al* [15] found that, if relaxation is taken into account, the appropriate value for t_4 should be 14. Thus, we use this last value for t_4 and the corresponding value for $\bar{b}_4(R_0)$ obtained by the same workers.

The values of t_2 and $\bar{b}_2(R_0)$ can be obtained from strain data of single oxides. Newman and Siegel [18] and Siegel and Müller [19] use the values obtained by this method. However, they assumed that the value of the distance R_0 corresponding to the obtained $\bar{b}_2$ is half the lattice constant of the host. On the contrary, it is clear at present that there is a relaxation of the single-oxide lattice around the impurity [15, 20]; so the actual value for the distance should be used. In summary, we have used the $\bar{b}_2$-value of $-0.157\ cm^{-1}$ [19] from the strain data of MgO and the relaxed R_0-value of 2.1463 Å [15] instead of 2.1 Å (which is half the MgO lattice constant) for the Mn^{2+}–O^{2-} distance.

By using the previously discussed values for $\bar{b}_2$, t_2, $\bar{b}_4$ and t_4 and assuming that in $Bi_4Ge_3O_{12}$ there is no relaxation of the oxygen ligands, i.e. that $R_a = 2.149$ Å, R_b = 2.620 Å, $\theta_a = 51.38°$ and $\theta_b = 104.62°$, we obtain $b_2^0 = +78.7 \times 10^{-4}\ cm^{-1}$, which is completely different from the experimental value of $-52.2 \times 10^{-4}\ cm^{-1}$. Also, the values obtained for b_4^0 and b_4^3 are very different from the experimental values. Thus, it is clear that, as we proposed before in the discussion of the value of A_s, the oxygen ligands cannot be in the normal position in the lattice; they must undergo some relaxation.

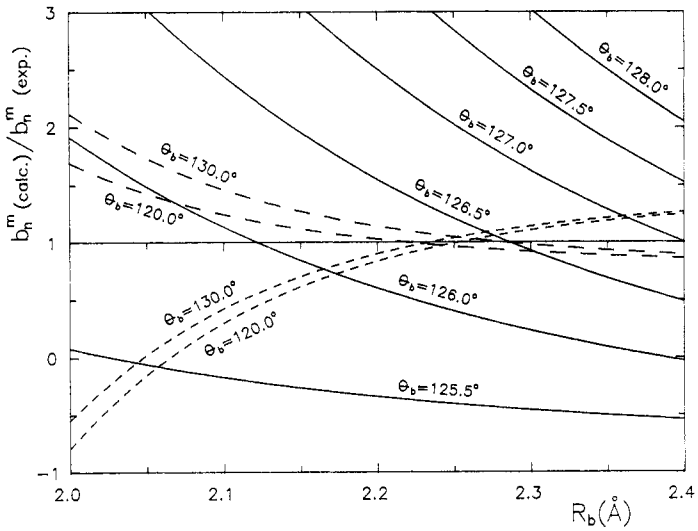

Figure 4. Plot of the ratios b_n^m(calc)/b_n^m(exp) in the case of b_2^0 (——), b_4^0 (– – –) and b_4^3 (- - -), calculated with fixed values of parameters $R_a = 2.06$ Å and $\theta_a = 55°$, as a function of R_b for different values of θ_b indicated next to the curves. See text for explanation.

By considering the behaviour of the $K_4^0(\theta, \varphi)$ function, we ascertain that the only way to obtain values for b_4^0 close to the experimental value is to decrease strongly the distance R_b. Then, we can assume some fixed values for R_a and θ_a (similar to those of the unrelaxed lattice) and obtain the ratios b_n^m(calc)/b_n^m(exp) by scanning R_b for different values of θ_b. In this way, we obtain the set of curves shown in figure 4. The pair of values for R_b and θ_b that yields a value of about unity for the three ratios constitutes a solution. Next, we can modify the values of R_a and θ_a within a certain range in order to obtain the best fitting of the experimental values of b_n^m. It is obvious that there is not a single solution but there is a short interval in which the possible values of the variables must lie. In fact, $R_a = 2.1 \pm 0.05$ Å, $R_b = 2.2 \pm 0.1$ Å, $\theta_a = 55° \pm 5°$ and $\theta_b = 125° \pm 9°$. Moreover, it is found that, if R_a is decreased, R_b must be increased.

These results imply that the ligands around the Mn^{2+} ion strongly relax in such a way that the neighbourhood tends to form an almost regular octahedron of MnO_6^{10-}, although this octahedron is slightly distorted because of the host lattice where it is embedded. This conclusion is in agreement with the work by Souiri *et al* [21]. These workers have pointed out that a given pair of bonded ions has the tendency to maintain its bond length, constant, independent of the host matrix, and that this length is similar to that in the corresponding binary compound.

Acknowledgments

This work has been supported by Comisión Interministerial de Ciencia y Tecnología under project MAT88-0431-C02-01 and fundación R Areces.

References

[1] Grabmaier B G 1984 *IEEE Trans. Nucl. Sci.* **NS-31** 372–6
[2] Kurz S K and Perry T T 1968 *J. Appl. Phys.* **39** 3798–813
[3] Kaminskii A A, Sarkisov S E, Butaeva T I, Denisenko G A, Hermoneit B, Bohm J, Gosskrentz W and Schultze D 1979 *Phys. Status Solidi* a **56** 725–36
[4] Moya E, Contreras L and Zaldo C 1988 *J. Opt. Soc. Am.* B **5** 1737–42
[5] Kurz H 1974 *Ferroelectrics* **8** 437–9
[6] Schunemann P G, Temple D A, Hatchcock R S, Tuller H L, Jenssen H P, Gabbe D R and Warde C 1988 *J. Opt. Soc. Am.* B **5** 1685–96
[7] Segal D J, Santoro R P and Newnham R E 1966 *Z. Kristallogr.* **123** 73–6
[8] Kaminskii A A, Schultze D, Hermoneit B, Sarkisov S E, Li L, Bohm J, Reiche P, Ehlert R, Mayer A A, Lomonov V A and Balashov V A 1976 *Phys. Status Solidi* a **33** 737–53
[9] Jiménez E, Arizmendi L and Cabrera J M 1988 *J. Phys. C: Solid State Phys.* **21** 1299–305
[10] Blanzat B, Raynal F, Parrot R, Barthou C and Canny B 1976 *Phys. Status Solidi* b **76** K5–8
[11] Serway R A, Berlinger W, Müller K A and Collins R W 1977 *Phys. Rev.* B **16** 4761–8
[12] Van Wieringen J S 1955 *Discuss. Faraday Soc.* **19** 118–26
[13] Matumura O 1959 *J. Phys. Soc. Japan* **14** 108–14
[14] Simánek E and Müller K A 1970 *J. Phys. Chem. Solids* **31** 1027–40
[15] Rubio J O, Murrieta H S and Aguilar G S 1979 *J. Chem. Phys.* **71** 4112–22
[16] Newman D J 1971 *Adv. Phys.* **20** 197–259
[17] Newman D J 1975 *J. Phys. C: Solid State Phys.* **8** 1862–8
[18] Newman D J and Siegel E 1976 *J. Phys. C: Solid State Phys.* **9** 4285–92
[19] Siegel E and Müller K A 1979 *Phys. Rev.* B **19** 109–20
[20] Rubio J O, Chen Y and Abraham M M 1977 *J. Phys. Chem. Solids* **38** 215–6
[21] Souiri M, Goltzene A and Schwab C 1986 *Phys. Status. Solidi* b **138** 321–30